

Probing the thiol-gold planar interface by spin polarized tunneling

Xiaohang Zhang, Stephen A. McGill, Peng Xiong, Xiaolei Wang, and Jianhua Zhao

Citation: *Applied Physics Letters* **104**, 152403 (2014); doi: 10.1063/1.4871585

View online: <http://dx.doi.org/10.1063/1.4871585>

View Table of Contents: <http://scitation.aip.org/content/aip/journal/apl/104/15?ver=pdfcov>

Published by the [AIP Publishing](#)

Articles you may be interested in

[Spin-transfer force acting on vortex induced by current gradient in a planar polarizer geometry](#)

J. Appl. Phys. **114**, 113911 (2013); 10.1063/1.4822020

[Macrospin model of precessional spin-transfer-torque switching in planar magnetic tunnel junctions with perpendicular polarizer](#)

Appl. Phys. Lett. **102**, 152413 (2013); 10.1063/1.4802720

[Interface charge transfer in polypyrrole coated perovskite manganite magnetic nanoparticles](#)

J. Appl. Phys. **111**, 044309 (2012); 10.1063/1.3686662

[In-plane stray field induced spin-filtering in a two-dimensional electron gas under the modulation of surface ferromagnetic dual-gate](#)

J. Appl. Phys. **108**, 073703 (2010); 10.1063/1.3490780

[Spin polarized tunneling as a probe for quantitative analysis of field dependent domain structure in magnetic tunnel junctions](#)

J. Appl. Phys. **89**, 6668 (2001); 10.1063/1.1361044

An advertisement for the 'Physics Today' comment feature. It features a blue background with the 'physicstoday' logo in white. Below the logo, the text 'Comment on any Physics Today article.' is written in a large, white, serif font. To the right, there is a collage of images showing a 'Physics Today' article titled 'Measured energy in Japan' and a 'Comment on this article' box. A red arrow points from the article to the comment box. The comment box contains text discussing the article's findings and calculations.

Probing the thiol-gold planar interface by spin polarized tunneling

Xiaohang Zhang,^{1,a)} Stephen A. McGill,^{1,b)} Peng Xiong,^{1,c)} Xiaolei Wang,² and Jianhua Zhao²

¹Department of Physics, Florida State University, Tallahassee, Florida 32306, USA

²State Key Laboratory of Superlattices and Microstructures, Institute of Semiconductors, Chinese Academy of Sciences, P.O. Box 912, Beijing 100083, China

(Received 13 January 2014; accepted 4 April 2014; published online 16 April 2014)

Reports of induced magnetism at thiol-gold interface have generated considerable recent interest. In these studies, the sample magnetization was generally measured by superconducting quantum interference device magnetometry which has limitation in determining surface and interface magnetism. In this work, we have fabricated planar tunnel junctions incorporating a thiol-gold interface. An observed room temperature humidity effect together with low temperature inelastic electron tunneling spectroscopy confirmed the existence of a thiol-gold interface in the organic-inorganic hybrid heterostructure. Spin polarized tunneling measurements were performed to probe the spin polarization at the thiol-gold interface; however, the obtained spin polarized tunneling spectra indicate no measurable spin polarization at the thiol-gold interface. © 2014 AIP Publishing LLC. [<http://dx.doi.org/10.1063/1.4871585>]

The decoration of inorganic metals and semiconductors with organic self-assembled monolayers (SAMs) has led to surfaces that exhibit emergent physical properties and functionalities. Examples of these functionalities include modified wettability,¹ reduced friction,² and even bioactivity enabled by monolayers formed from biological materials like DNA.³ Furthermore, hybrid organic-inorganic constructions also provide a promising route towards the bottom-up assembly of functional nanostructures since covalently linked organics can self-assemble on inorganic nanoparticles and nanowires. Molecular electronics already takes advantage of hybrid organic-inorganic design to study electron transport through molecular monolayers as well as single molecules.^{4,5} During the last decade, there has been increased interest in incorporating organic molecules in spintronic devices.^{6–8} Although inorganic magnetic materials are presently an essential ingredient in most of such devices, there is much recent effort to produce magnetic responses in devices without any ferromagnetic materials. Most recent examples include spin filtering in carbon nanostructures⁹ and generation of polarized spins in nonmagnetic metals and semiconductors by the spin Hall effect.¹⁰ Another promising route to this goal is via surface modification of nonmagnetic metals by organic SAMs. The latter approach was bolstered by recent observations of induced magnetic moments, even ferromagnetism, at thiol-metal interfaces.^{11,12} Such hybrid structures can be readily integrated into spintronic devices and potentially used as a functional component for spin injection and detection.

In recent years, several groups have reported experimental observations of induced magnetism at thiol-functionalized gold surfaces.^{11,12} Carmeli *et al.*¹¹ reported highly unusual

induced magnetism in Au thin films functionalized with thiolated molecules. With an applied magnetic field perpendicular to the interface, a strong paramagnetic response with negligible temperature dependence was found and the measured moment is estimated to exceed *several tens of Bohr magnetons per adsorbed molecule*. Although the magnetization is found to be anisotropic, the magnetic moment is still significant in a parallel field of 1 T. A series of work from the group show high spin selectivity at room temperature for electron transfer through chiral molecules such as double-stranded DNA self-assembled on gold thin films.¹³ However, theoretical explanation of the extraordinary magnetic properties observed on such two-dimensional (2D) interfaces remains controversial.^{14,15} Experimentally, induced magnetism has been studied extensively in gold nanoparticles (NPs) decorated with organic molecules, but the results are not always consistent. Crespo *et al.*¹² shows that the magnetism of thiol-capped gold NPs is ferromagnetic, while similar gold NPs with a weakly interacting capping layer do not show noticeable magnetism. A later study¹⁶ by the same group indicates that contribution from Fe impurities can be ruled out as the origin of the observed ferromagnetism. On the other hand, earlier superconducting quantum interference device (SQUID) measurements by Hori *et al.*¹⁷ reveal that gold NPs functionalized with covalently bonded dodecanethiol show minimal magnetism in comparison to NPs decorated with weakly interacting molecules; X-ray magnetic circular dichroism (XMCD) results from Yamamoto *et al.*¹⁸ indicate a significant ferromagnetic spin polarization on gold NPs with a diameter of 1.9 nm capped with a weakly interacting polymer, polyallylamine hydrochloride. More recently, investigations by XMCD and Mössbauer spectroscopy indicate permanent magnetism is induced not only in thiol-capped gold NPs but also in silver and copper NPs synthesized by the same chemical procedure.¹⁹

Despite the apparently inconsistent experimental results and the still controversial understanding of the physical mechanism, broad interest has been stimulated by these

^{a)}Current address: Center for Nanophysics and Advanced Materials, University of Maryland, College Park, Maryland 20742, USA.

^{b)}Current address: National High Magnetic Field Laboratory, Florida State University, Tallahassee, Florida 32310, USA.

^{c)}Electronic mail: xiong@physics.fsu.edu

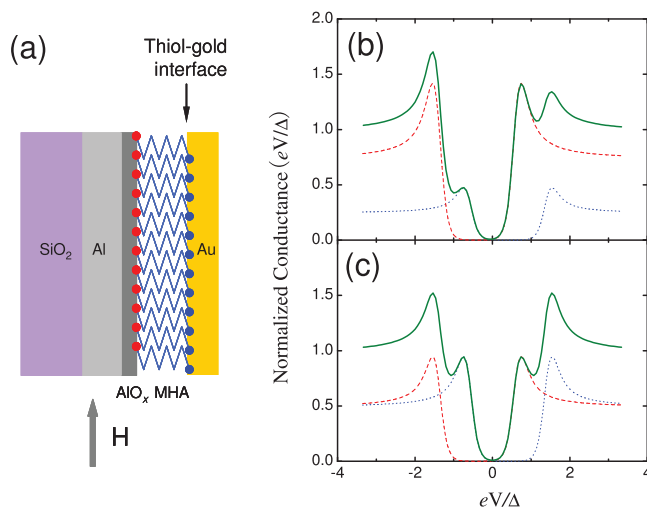


FIG. 1. (a) Schematic side-view of the cross-section of an Al/AIO_x/MHA/Au junction at the junction area (not to scale). An external magnetic field is applied parallel to the planar interfaces in the junction. (b) and (c) illustrate the expected Zeeman-resolved tunneling spectra: for a magnetic thiol-gold interface, an asymmetric spectrum (b) is expected; however, if the interface is non-magnetic, the spectrum is symmetric as shown in (c). The solid curves are the normalized conductance spectra; while the dashed and the dotted curves, respectively, represent contributions from spin-up and spin-down currents.

reports primarily due to the potential applications in molecular spintronics. For example, the giant magnetic moments of tens of Bohr magnetons at the thiol-gold interface could be utilized as effective spin filters in a small magnetic field, thus may be applicable for spin injection. As the most ubiquitous organic/metal interface, thiol/Au can be easily integrated into device structures. For the purpose of exploring spintronic applications, it is essential to integrate the interface into a device structure while preserving its magnetism and spin filtering effect. On the other hand, most measurements of the induced magnetism to date has been conducted by volume-based or surface-sensitive techniques, which often have complications^{20,21} and may not be applicable to a buried interface. Motivated by these reasons, we attempt to directly investigate the spin dependent density of states (DOS) at 2D thiol-gold interfaces using the spin-polarized electron tunneling technique.²²

The fabrication of planar tunnel junctions incorporating a layer of mercaptohexadecanoic acid (MHA) between gold

and surface-oxidized Al contacts has been reported elsewhere.²³ The thickness of the Al layer was controlled to be about 50 Å in junctions used for spin polarized tunneling (SPT) study while about 700 Å in junctions fabricated for inelastic electron tunneling spectroscopy (IETS) measurements to avoid current crowding at high bias. The finished junctions had a structure of Al/AIO_x/MHA/Au (Fig. 1(a)) and an area of approximately 0.4 × 0.4 mm².

The SPT technique, invented by Meservey and Tedrow in early 1970s, is a method to determine the spin polarization of a material from a Zeeman-split superconducting tunneling spectrum. Frequently, a thin Al layer is used as the superconductor electrode because of the high in-plane critical field and small spin-orbit coupling. For example, an Al film with a thickness of 4 nm will remain in the superconducting state in an in-plane magnetic field as large as 4 T.²⁴ Such a high critical magnetic field ensures significant Zeeman splitting of the quasiparticle DOS, leading to a spin resolved tunneling spectrum. Specifically for our junctions, if sufficiently large magnetic moments are induced by thiol-gold bonds and are further aligned in an external magnetic field, the interface would effectively work as a spin filter for the tunneling current and eventually result in an asymmetric conductance spectrum as illustrated in Fig. 1(b); however, in the case that no or very small magnetic moments are induced at the interface, the spin polarization is expected to be effectively zero for the junction structure while the conductance spectrum shows symmetric peaks (Fig. 1(c)).

Temperature dependence of the junction resistance (R_J) and electron tunneling spectra were obtained in a He³ cryostat (Oxford) with an 8-T superconductor magnet. The conductance spectrum was measured via first-harmonic phase-sensitive detection at a frequency of 17.3 Hz using a PAR124A lock-in amplifier and a home-made DC voltage sweeper. Fig. 2(a) shows the temperature dependence of the resistance for an Al/AIO_x/MHA/Au junction. As the temperature decreases, the zero-bias junction resistance exhibits a very weakly insulating temperature dependence with $R_J(300\text{ K})/R_J(4\text{ K}) \sim 0.96$, which is a typical characteristic of a tunnel junction. At about 2.0 K, the thin Al layer enters the superconducting phase and the formation of the energy gap leads to a dramatic increase in the zero-bias junction resistance. At the base temperature of the cryostat (0.35 K), the junction resistance reaches a value of ~ 33 times of $R_J(4\text{ K})$.

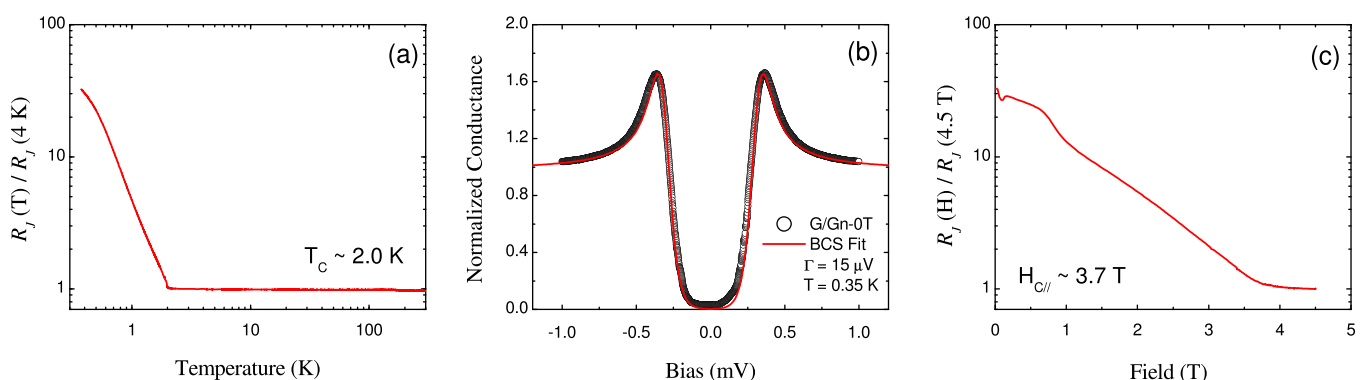


FIG. 2. (a) Temperature dependence of the zero-bias junction resistance for an Al/AIO_x/MHA/Au junction; (b) Zero-field normalized conductance curve of the junction and a BCS fitting with an inelastic scattering term of 15 μV; (c) Zero-bias junction resistance as a function of the applied magnetic field at 0.35 K for the same junction.

For the purpose of investigating SPT in these junctions, this junction resistance ratio, $R_J(0.35\text{ K})/R_J(4\text{ K})$, and the T_C of the Al layer are two important factors. Fig. 2(b) shows the zero-field conductance curve, normalized with a high-field spectrum at the same temperature, as a function of bias voltage at 0.35 K for the same junction. The solid curve in Fig. 2(b) indicates a theoretical fit to the Bardeen-Cooper-Schrieffer (BCS) superconducting DOS with a negligible lifetime broadening²⁵ of $15\ \mu\text{eV}$. Both the subgap conductance and the lifetime broadening of the junction are similar to an identically fabricated Al/AIO_x/Au junction without the MHA layer. These results provide definitive evidence of high-quality electron tunneling in the Al/AIO_x/MHA/Au junction.

To verify the covalent bonding at the thiol-gold interface, we have also performed IETS measurements on junctions identically fabricated but with much thicker Al electrodes. The results have been reported in Ref. 23. The observation of peaks corresponding to vibration modes of C-S, CH₂, OH, and Au-S bonds in the spectrum, combined with the absence of the feature for the S-H bond at $\sim 320\text{ meV}$,²⁶ suggests that most of the thiol end groups of the MHA had reacted with the Au layer. Another important observation in these Al/AIO_x/MHA/Au junctions is that the junction resistances are highly sensitive to the surrounding atmosphere at room temperature. Such variations in junction resistance are not observed in samples without the monolayer and systematic studies²³ have revealed that this behavior is essentially corresponding to changes of the tunneling barrier height upon dehydration or hydration of the MHA/AIO_x interface. The observed humidity effects on the junction resistance, together with the IETS results, indicate that direct elastic tunneling dominates the electron transport in these devices and the tunneling behavior does involve the MHA monolayer.

To obtain the spin dependent tunneling spectrum, a magnetic field was applied parallel to the Al layer. The alignment of the film plane with the applied magnetic field was adjusted *in situ* to obtain optimal results. Fig. 2(c) shows the zero bias junction resistance versus the applied magnetic field at 0.35 K. The junction resistance decreases with increasing field, and eventually flattens out above 3.7 T which was determined as the critical field of the Al layer. The critical fields of our samples were found to range from 3.6 T to 4.0 T, suggesting a well controlled thickness for the Al layer²⁴ and a near-perfectly aligned external magnetic field. Fig. 3(a) shows the normalized conductance spectra at several magnetic fields. At a magnetic field above 3 T, the conductance spectrum was clearly Zeeman resolved, leading to a spin dependent spectrum. However, the four peaks on the spectrum remain symmetric as in the case in Fig. 1(c), suggesting there is no discernible spin polarization from the thiol-gold interface. Fig. 3(b) displays the conductance spectra of a sample that was almost identically fabricated as the one shown in Fig. 3(a), with the only exception that the MHA self-assembling procedure²⁵ was replaced by immersing the Al film into pure ethanol for the same length of time. This sample showed a much lower junction resistance than the one with the monolayer, and as also expected from the junction structure, symmetric Zeeman resolved conductance spectra were obtained. The results conclusively demonstrate

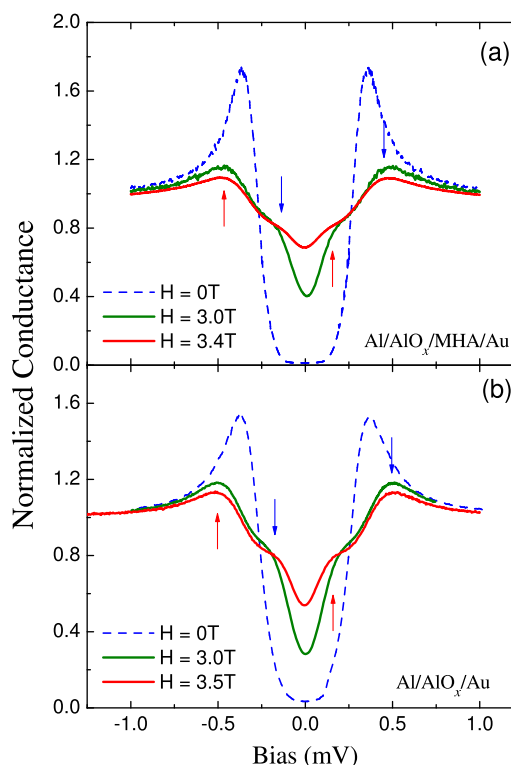


FIG. 3. Spin polarized tunneling spectra of (a) an Al/AIO_x/MHA/Au junction and (b) an Al/AIO_x/Au junction at 0.35 K. Zeeman-resolved peaks are indicated by arrows with the directions correspond to the spin states.

that although the existence of the MHA monolayer in the junction structure significantly increases the junction resistance, it does not change the spin-polarized tunneling results, i.e., the thiol-gold interface does not induce a measurable spin-polarized tunneling current. Several Al/AIO_x/MHA/Au junctions have been fabricated and measured in this manner; none of them displayed any evidence of a non-zero spin polarization at the thiol-gold interface.

SPT technique is a sensitive measurement in probing spin polarization of materials. For instance, a spin polarization of less than 5% can be easily determined by this method with an accuracy of 1%.²⁷ In our measurements, although the determined magnitude of the spin polarization at the 2D thiol-gold interface is less than 1%, the result does not necessarily indicate the lack of induced magnetism; instead, our measurements suggest that even giant magnetic moments are present at the interface, the structure cannot produce a spin current with a sufficiently high spin polarization, thus is not likely to be applicable for spin injection. To definitively determine the magnetism at the 2D thiol-gold interface due to potential experimental complications,^{20,21} other interface-magnetism-sensitive measurements are still highly desirable.

In summary, we have fabricated tunnel junctions that incorporate a superconducting electrode and an organic SAM layer in the barrier. The superconducting tunneling spectroscopy results indicated that the junctions are high-quality tunnel junctions with negligible inelastic broadening. The IETS results and a pronounced repeatable humidity effect further verified the existence of the monolayer in the junction structure and confirmed the specific bonding of thiol-gold. Spin-polarized tunneling measurements have

been successfully performed; however, the results did not show any evidence of a non-zero spin polarization at the 2D thiol-gold interface.

This work was supported by NSF Grant No. DMR-1308613 and NSFC Grant No. 11228408.

- ¹P. E. Laibinis and G. M. Whitesides, *J. Am. Chem. Soc.* **114**, 1990 (1992).
²V. V. Tsukruk and V. N. Bliznyuk, *Langmuir* **14**, 446 (1998).
³L. M. Demers, D. D. Ginger, S. J. Park, Z. Li, S. W. Chung, and C. A. Mirkin, *Science* **296**, 1836 (2002).
⁴C. Joachim and M. Ratner, *Proc. Natl. Acad. Sci. U. S. A.* **102**, 8801 (2005).
⁵M. Ratner, *Nat. Nanotechnol.* **8**, 378 (2013).
⁶C. Herrmann, G. C. Solomon, and M. A. Ratner, *J. Am. Chem. Soc.* **132**, 3682 (2010).
⁷S. Sanvito, *Chem. Soc. Rev.* **40**, 3336–3355 (2011).
⁸S. Steil, N. Großmann, M. Laux, A. Ruffing, D. Steil, M. Wiesenmayer, S. Mathias, O. L. A. Monti, M. Cinchetti, and M. Aeschlimann, *Nat. Phys.* **9**, 242 (2013).
⁹M. G. Zeng, L. Shen, Y. Q. Cai, Z. D. Sha, and Y. P. Feng, *Appl. Phys. Lett.* **96**, 042104 (2010).
¹⁰T. Jungwirth, J. Wunderlich, and K. Olejník, *Nature Mater.* **11**, 382 (2012).
¹¹I. Carmeli, G. Leitius, R. Naaman, S. Reich, and Z. Vager, *J. Chem. Phys.* **118**, 10372 (2003).
¹²P. Crespo, R. Litrán, T. C. Rojas, M. Multigner, J. M. de la Fuente, J. C. Sánchez-López, M. A. García, A. Hernando, S. Penadés, and A. Fernández, *Phys. Rev. Lett.* **93**, 087204 (2004).
¹³S. G. Ray, S. S. Daube, G. Leitius, Z. Vager, and R. Naaman, *Phys. Rev. Lett.* **96**, 036101 (2006).
¹⁴Z. Vager and R. Naaman, *Phys. Rev. Lett.* **92**, 087205 (2004); A. Hernando and M. A. García, *Phys. Rev. Lett.* **96**, 029703 (2006).
¹⁵B. Göhler, V. Hamelbeck, T. Z. Markus, M. Kettner, G. F. Hanne, Z. Vager, R. Naaman, and H. Zcharias, *Science* **331**, 894–897 (2011); Z. Xie, T. Z. Markus, S. R. Cohen, Z. Vager, R. Gutierrez, and R. Naaman, *Nano Lett.* **11**, 4652–4655 (2011).
¹⁶P. Crespo, M. A. García, E. Fernández Pinel, M. Multigner, D. Alcántara, J. M. de la Fuente, S. Penadés, and A. Hernando, *Phys. Rev. Lett.* **97**, 177203 (2006).
¹⁷H. Hori, Y. Yamamoto, T. Iwamoto, T. Miura, T. Teranishi, and M. Miyake, *Phys. Rev. B* **69**, 174411 (2004).
¹⁸Y. Yamamoto, T. Miura, M. Suzuki, N. Kawamura, H. Miyagawa, T. Nakamura, K. Kobayashi, T. Teranishi, and H. Hori, *Phys. Rev. Lett.* **93**, 116801 (2004).
¹⁹J. S. Garitaonandia, M. Insausti, E. Goikolea, M. Suzuki, J. D. Cashion, N. Kawamura, H. Ohsawa, I. G. de Muro, K. Suzuki, F. Plazaola, and T. Rojo, *Nano Lett.* **8**, 661 (2008).
²⁰J. Grace, M. Venkatesan, J. Alaria, J. M. D. Coey, G. Kopnov, and R. Naaman, *Adv. Mater.* **21**, 71 (2009).
²¹M. A. García, E. Fernandez Pinel, J. de la Venta, A. Quesada, V. Bouzas, J. F. Fernández, J. J. Romero, M. S. Martín González, and J. L. Costa-Krämer, *J. Appl. Phys.* **105**, 013925 (2009).
²²R. Meservey and P. M. Tedrow, *Phys. Rep.* **238**, 173 (1994).
²³X. H. Zhang, S. A. McGill, and P. Xiong, *J. Am. Chem. Soc.* **129**, 14470 (2007).
²⁴R. Meservey and P. M. Tedrow, *J. Appl. Phys.* **42**, 51 (1971).
²⁵R. C. Dynes, V. Narayanamurti, and J. P. Garno, *Phys. Rev. Lett.* **41**, 1509 (1978).
²⁶W. Wang, T. H. Lee, I. Kretschmar, and M. A. Reed, *Nano Lett.* **4**, 643 (2004).
²⁷R. Meservey, D. Paraskevopoulos, and P. M. Tedrow, *Phys. Rev. B* **22**, 1331 (1980).